

# On the dynamics near the Lagrangian points of the real Earth-Moon system

Enric Castellà and Àngel Jorba\*

Departament de Matemàtica Aplicada i Anàlisi

Universitat de Barcelona. Gran Via 585, 08007 Barcelona, Spain.

## Abstract

In this work we consider the motion of an infinitesimal particle near the equilateral points of the real Earth-Moon system. We use, as real system, the one provided by the JPL ephemeris: the ephemeris give the positions of the main bodies of the solar system (Earth, Moon, Sun and planets) so it is not difficult to write the vectorfield for the motion of a small particle under the attraction of those bodies. Numerical integrations of this vectorfield show that trajectories with initial conditions in a vicinity of the equilateral points escape after a short time.

On the other hand, it is known that the Restricted Three Body Problem is not a good model for this problem, since it predicts a quite large region of practical stability. For this reason, we will discuss a intermediate model that tries to account for the effect of the Sun. This model has some families of lower dimensional tori, that gives rise to a region of effective stability at some distance of the triangular points. It is remarkable that this region seem to persist in the real system, at least for time spans of 1000 years.

## 1 Introduction

One of the simplest models for this problem is the well known Restricted Three Body Problem (from now on, RTBP). The RTBP models the motion of a particle under the gravitational attraction of the Earth and Moon (also called primaries), under the following assumptions: i) the particle is so small that it does not affect the motion of Earth and Moon; and ii) Earth and Moon are point masses that revolve in circular orbits around their common centre of mass. It is well known [Sze67] that, in a rotating frame, the RTBP has five equilibrium points: three of them lay on the  $x$  axis (they are called collinear points,

---

\*Corresponding author. E-mail: [angel@maia.ub.es](mailto:angel@maia.ub.es)

Eulerian points, or simply  $L_{1,2,3}$ ), and the other two form an equilateral triangle (in the  $(x, y)$  plane) with Earth and Moon (they are called triangular points, Lagrangian points or simply  $L_{4,5}$ ). If the ratio of the masses of the primaries is small enough (this includes the Earth-Moon and Sun-Jupiter cases), the triangular points are linearly stable. Under very general conditions [GDF<sup>+</sup>89, Sim89, CG91, BFG98], there exists a neighbourhood of these points such that any initial condition inside this neighbourhood produces a trajectory that remains close to the point for huge intervals of time. This behaviour (stability for finite but very large time intervals) is also known as “effective stability”.

On the other hand, we can consider one of the most accurate models of the Solar system now available, which is the JPL Ephemeris [JPL]. Even if this model cannot be studied analytically, it can be integrated numerically. The main question is what features of the RTBP transfer to the JPL model. Clearly the Lagrangian points are not equilibrium points anymore when we take into account the real motion of Earth and Moon, and the presence of Sun and planets. Moreover, direct numerical integration of JPL model shows that the neighbourhood of the triangular points is no longer stable for the JPL model, since nearby trajectories escape after a short time [DJS91]. Therefore, the RTBP is not a good model to study this problem because it displays a quite different qualitative behaviour.

Since the discovery of the first Trojan asteroid near the Lagrangian points of the Sun-Jupiter system, there have been many unsuccessful searches for similar objects in the Earth-Moon system [FV80]. The main difference between these two cases is that Sun-Jupiter is closer to the RTBP, since the strong effect of the Sun puts the Earth-Moon case far from the RTBP model. For this reason, in the next Section we will introduce the so called Bicircular Problem (from now on, BCP). This model can be seen as a time dependent periodic perturbation of the RTBP, that includes the main effect coming from the Sun. As far as we know, this model was first published in [CRR64]. We will see that the BCP model has some of the main features of the real model (for instance, the neighbourhood of the equilateral points is unstable).

Our first goal will be to use the BCP to describe some properties of the real model. In particular, we will compute, for the BCP, families of quasi-periodic solutions near the equilateral points. We will see that some of them are unstable, while some others are stable. Those stable solutions are found at some distance from the equilateral points. It is known [JV97b, JV97a, JV01] that, under generic hypotheses, stable quasi-periodic solutions are surrounded by regions of effective stability. The size and shape of these regions will be estimated by means of numerical simulations. Finally, we will show, by means of numerical simulations, that some of these stability regions found in the BCP model seem to subsist in the JPL model, at least for time spans of 1000 years.

This kind of stability has been previously observed [GJMS93, GJMS01], but with

smaller regions and much shorter time intervals (around 60 years). The actual improvements come from a deeper study of the BCP to guess where these regions should be.

## 2 The Bicircular Problem

Let us assume that Earth and Moon are point masses that revolve in circular orbits around their common centre of mass (as in the RTBP), and let us also assume that this centre of mass revolves in a circular orbit around the Sun (also considered as a point mass) fixed at the origin. We are also assuming that the motion of the three bodies is coplanar. The purpose of the Bicircular Problem is the study of the motion of an infinitesimal particle under the attraction of these three main bodies. It is usual to take the same reference frame as in the RTBP. So, in this system of reference, Earth and Moon are fixed on the  $x$  axis while the Sun is turning around the Earth-Moon centre of masses, that is located at the origin. Therefore, we can look at the BCP as a periodic time dependent perturbation of the RTBP. In fact, we will write a parameter  $\varepsilon$  in front of the mass of the Sun so that, moving this parameter, our model goes from the RTBP ( $\varepsilon = 0$ ) to the BCP ( $\varepsilon = 1$ ).

Now, let us focus on the  $L_5$  point (due to the symmetries of the RTBP and BCP, the same results will hold for  $L_4$ ; of course, this does not apply to the real system). As the vector field of the BCP does not vanish on  $L_5$ , this point is not longer an equilibrium solution. It is not difficult to prove that, under a generic non-resonance condition (satisfied in this case) and assuming  $\varepsilon$  small enough,  $L_5$  is replaced by a periodic orbit with the same period as the perturbation. This orbit tends to  $L_5$  when  $\varepsilon$  tends to zero.

Let us consider now the Poincaré section defined by  $t = 0(\text{mod } T_S)$ , where  $T_S$  is the period of the time-dependence (i.e., the Sun) in the BCP and let us call  $P_\varepsilon$  the corresponding Poincaré map. Now, let us compute the fixed points of  $P_\varepsilon$  for  $\varepsilon$  ranging between 0 and 1. The results are displayed in Figure 1 (left), where the horizontal axis shows the  $x$  coordinate of the fixed point and the vertical axis refers to the value of  $\varepsilon$ . Note that, for  $\varepsilon = 1$  (the BCP), there are three fixed points of  $P_\varepsilon$  that are close to  $L_5$ . The  $(x, y)$  projection of the corresponding periodic orbits for the flow are displayed in Figure 1 (right). It is easy to see that orbit PO1 is unstable, while orbits PO2 and PO3 are linearly stable. Moreover, the three periodic orbits have an elliptical mode contained in the  $(z, \dot{z})$  plane (this corresponds to librations perpendicular to the plane of motion of the Moon around the Earth). In what follows, we will refer to this mode as the vertical mode of the corresponding periodic orbit. For more details about the BCP we refer to [GJMS93, SGJM95, GJMS01].

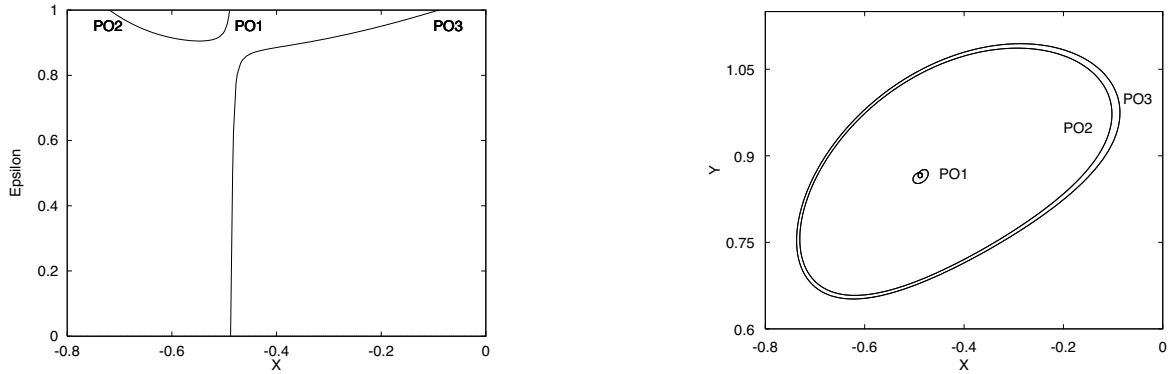


Figure 1: Left: Continuation of the periodic orbit that replaces  $L_5$  in the BCP. Right: The three periodic orbits that appear on the left plot for  $\varepsilon = 1$ .

### 3 Families of quasi-periodic motions in the BCP

As mentioned before,  $L_5$  is a linearly stable equilibrium point of the RTBP. Moreover, the linearization of the vector field at this point can be described as the product of three linear oscillators: two of them are contained in the  $(x, y)$  plane, and the third one moves exactly on the  $z$  axis. In what follows, let us focus on this vertical oscillation of the RTBP that is contained in the  $z$  axis. The well-known Lyapunov centre theorem implies that this vertical oscillation of the linearized system can be extended into the complete RTBP, giving rise to a family (the Lyapunov family) of periodic orbits, that we will refer to as the vertical family.

Let us look at the BCP as a (periodic) perturbation of the RTBP. If the perturbing parameter  $\varepsilon$  is small enough, we have already mentioned that  $L_5$  becomes a small periodic orbit (with the frequency of the Sun in the BCP). Moreover, it is known [JV97b] that the vertical family of periodic orbits becomes a (Cantor-like) family of quasi-periodic orbits, that will be called the vertical family of quasi-periodic solutions. These solutions have two basic frequencies: the first coming from one of the periodic orbits of the vertical family and the second being the frequency of the Sun. Let us consider the periodic orbits of the BCP for  $0 < \varepsilon \leq 1$  (see Figure 1). It can also be proved [JV97a] that the linear vertical mode of these periodic orbits can be extended into the full (nonlinear) system, as a (Cantor) family of quasi-periodic solutions. For definiteness, when  $\varepsilon = 1$ , we will call VF1, VF2 and VF3 to the vertical families born in PO1, PO2 and PO3 respectively.

These three families can be accurately computed by means of numerical methods [CJ00, Jor01]. The results for  $\varepsilon = 0.91$  and 1 are shown in Figure 2. Note that the families VF1 and VF2 are connected, as it is suggested by the diagram in Figure 1 (left). The gaps that conform the Cantor structure of these curves are too small to be seen at this scale.

As PO1 is unstable, we expect that the tori in VF1 are also unstable, at least for moderate values of the vertical amplitude. PO2 and PO3 are stable orbits so, under

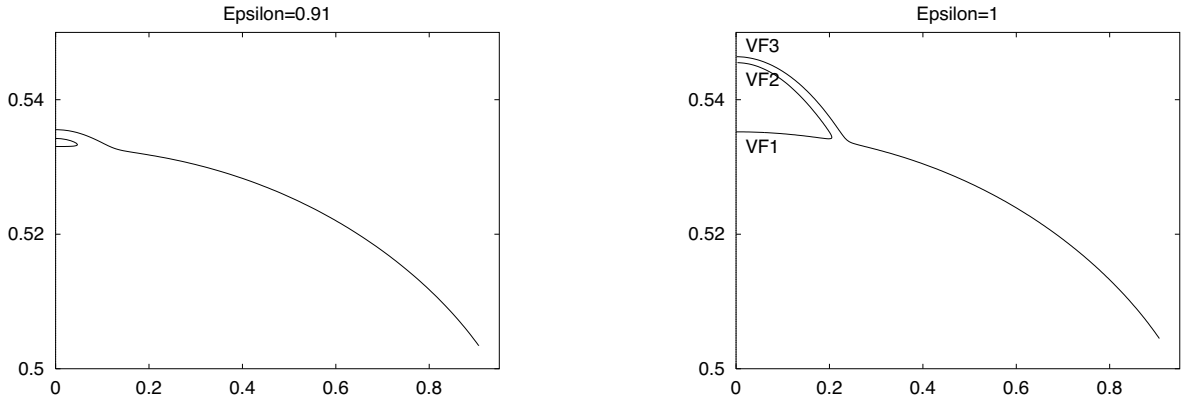


Figure 2: Vertical families of invariant tori for  $\varepsilon = 0.91$  and 1. The horizontal axis shows the value of the coordinate  $\dot{z}$  of the invariant curve when  $t = 0$  and  $z = 0$ , and the vertical axis shows the corresponding rotation number.

generic conditions, it is expected that most of the tori in families VF2 and VF3 with a small vertical amplitude are also stable (it is also expected that a few of them are unstable due to resonances).

#### 4 Stability regions in the BCP

As it has been mentioned before, a stable quasi-periodic trajectory is surrounded by a region of effective stability. Here we will try to estimate this region by means of a numerical simulation. To select a mesh of initial conditions around a given solution, let us consider the map  $P_\varepsilon$  defined before. Note that a (vertical) quasi-periodic solution corresponds to an invariant circle of  $P_\varepsilon$  that crosses transversally the plane  $z = 0$  in two points, with different signs for  $\dot{z}$ . So, let us select the (unique) point on the invariant curve having  $z_0 = 0$  and  $\dot{z}_0 > 0$  (this value of  $\dot{z}_0$  is, in fact, the value displayed on the vertical axis of Figure 2). In this way, we select a unique point on each quasi-periodic solution.

The mesh used is of the kind  $(x_{ij}, y_{ij}, 0, \dot{x}_0, \dot{y}_0, \dot{z}_0)$ , where the values  $(\dot{x}_0, \dot{y}_0, \dot{z}_0)$  correspond to a given quasi-periodic solution (see above), and  $x_{ij}$  and  $y_{ij}$  are distributed around the corresponding values  $(x_0, y_0)$ . In fact, these values are taken as  $x_{ij} = r_i \cos \alpha_j + \mu$ ,  $y_{ij} = r_i \sin \alpha_j$ , where  $r_i$  and  $\alpha_j$  are equally spaced. Then, we numerically integrate the trajectories of the BCP starting on each point of the mesh. If the trajectory does not cross the  $y = -0.5$  plane, and does not approach collision neither with Earth nor Moon during the integration time, we take the initial condition as belonging to the stability region. Note that, in this way, we produce a 2-D slice instead of the full region.

We have done an extensive numerical simulation for the trajectories in the families VF2 and VF3 (they mostly contain linearly stable tori), during a time interval of 15000 revolutions of the Moon around the Earth. The results show the existence of large stability regions [Jor00]. Here we will only focus on the family VF3, since the corresponding regions

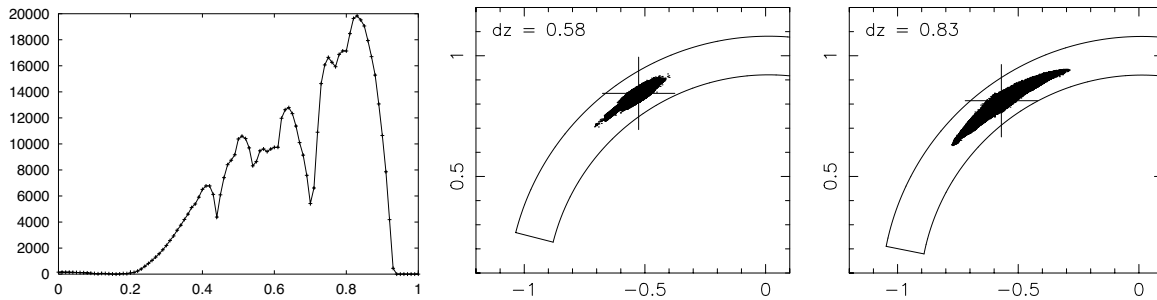


Figure 3: Size of the stability region for the VF3 family of the BCP. First plot: value of the  $\dot{z}$  coordinate vs. the number of initial conditions inside the region. Second and Third plots: Computed stability region for the BCP, for the cases  $\dot{z} = 0.58$  (2nd) and  $\dot{z} = 0.83$  (3rd). The initial quasi-periodic solution is marked with a big “+” sign.

are bigger. These results are summarized in Figure 3. As the mesh has the same size in all the cases, the number of initial conditions corresponding to non-escaping trajectories is a good estimate for the size of the region. Note that the region is neglectable when  $\dot{z} < 0.23$  or  $\dot{z} > 0.93$ . The boundary of these regions is quite sharp, and they are almost not affected by an increasing of the integration time. This phenomenon is known to happen in similar situations [SGJM95].

To show the shape of these regions, Figure 3 shows (slices for) a couple of regions,  $\dot{z} = 0.58$  and  $\dot{z} = 0.83$ . Both plots display the  $(x, y)$  coordinates of the points in these regions. The explored region has been marked with a semi-circular box.

## 5 Stability regions in the JPL model

A natural question is whether these regions persist in the real system. To this end, we have repeated the above simulations around the family VF3 using the JPL ephemeris (file DE406), for a time interval of 1000 years. Here, the initial integration time is the first full Moon of year 2000 (this is to have a relative position of Earth, Moon and Sun similar to the one of the BCP when  $t_{BCP} = 0$ ).

The results are summarized in Figure 4. Note that the JPL model does not have the above-mentioned symmetries between the triangular points so we have different plots for them. The horizontal axis refers to the  $\dot{z}$  coordinate of the torus in the Poincaré section  $P_\varepsilon$  of the BCP, as it has been previously introduced. The vertical axis contains the number of points of the initial mesh that do not escape after several time intervals, ranging from 500 to 1000 years. As all the meshes used have the same density, the number of surviving points can be considered an estimate on the size of the stable region. In this case, the boundaries of the stability region are not as sharp as in the BCP case (there is a small but noticeable leaking of stable initial conditions when the integration time increases).

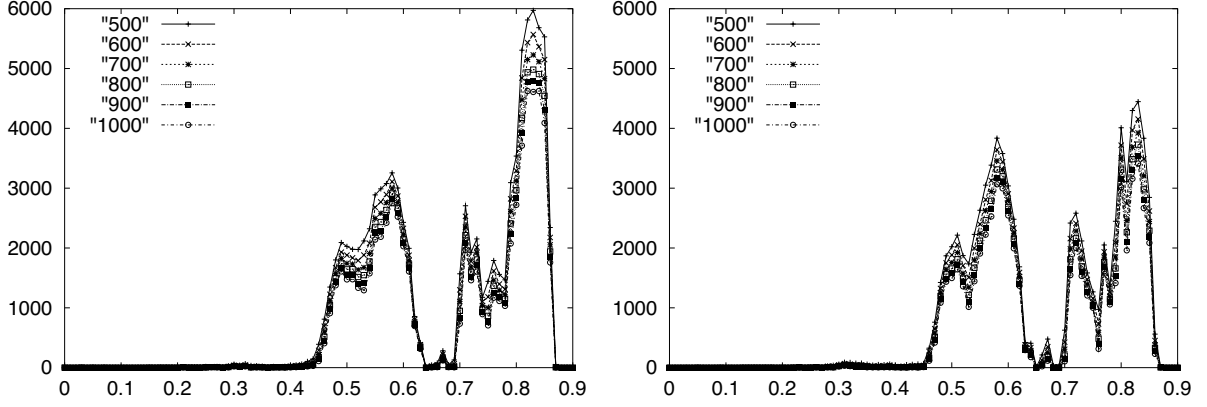


Figure 4: Size of the stability region in the JPL model, for  $L_4$  (left) and  $L_5$  (right). Horizontal axis: value of the  $z$  coordinate. Vertical axis: number of non-escaping initial conditions.

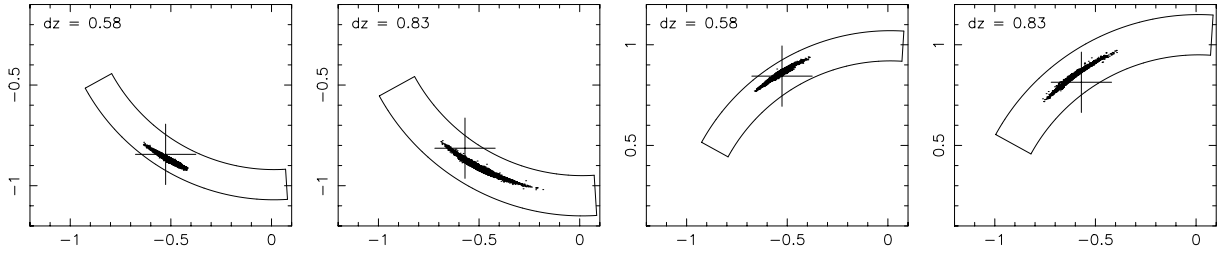


Figure 5: Stability region for the JPL model, for  $L_4$  and  $z = 0.58$  (1st plot), for  $L_4$  and  $z = 0.83$  (2nd plot), for  $L_5$  and  $z = 0.58$  (3rd plot) and for  $L_5$  and  $z = 0.83$  (4th plot). The box corresponds to the explored region. The initial condition corresponding to the quasi-periodic solution is marked with a big “+” sign.

The shape of these regions is determined by several phenomena; but probably the most important one is due to resonances between the relevant frequencies. It also clear that the BCP does not display all the features of the real system, probably because it does not take into account all the important frequencies. The obtention of a better model as well as a complete study of the resonances involved is actually work in progress.

Note that, according to Figure 4, the stability region has a relevant size for the values  $z = 0.58$  and  $z = 0.83$ . In these simulations, we have used the same mesh as in the BCP problem, so it is possible to compare the sizes of these regions. Although there is a strong reduction in size, the number of remaining points is still significative. Figure 5 shows the results of the simulations for the cases  $z = 0.58$  and  $z = 0.83$ . As before, the horizontal ( $x$ ) and vertical ( $y$ ) axis are RTBP coordinates (that is, the unit of distance is the Earth-Moon distance).

## 6 Conclusions

The main purpose of this work has been to show the existence of regions of practical stability near the equilateral points of the real Earth-Moon system. The methodology is based on obtaining a first guess for these regions by applying very recent results and techniques from Hamiltonian dynamical systems to a suitable intermediate model (the BCP). These regions are tested numerically on a realistic model of the Solar system obtained from the JPL ephemeris. In this way, we avoid doing massive numerical simulations on the JPL model that could result in a prohibitive need of computer time.

A natural question is the persistence of these regions for much longer time intervals. We are actually working in this direction by using improved versions of the BCP, taking into account Moon's eccentricity and Sun's inclination. The results for these models will be tested against longer numerical integrations of the Solar system. This is actually work in progress.

The motion for a particle in this region is shown in Figure 6. To give a sense of velocity we have drawn the orbit as a polygonal line, putting a vertex for each (Julian) day of integration. From Figure 4 it is clear that the largest part of the region corresponds to trajectories that cut the Earth-Moon plane with vertical speeds (relative to that plane) close to either 0.58 or 0.83, in adimensional units. This corresponds to speeds close to either 0.56 or 0.80 Km/sec. From the  $(z, \dot{z})$  projections shown in Figure 6, it is clearly seen that the motion in the vertical direction is very close to an harmonic oscillator (with a period of a little less than a month), and that these trajectories reach an approximate angular separation over (or under) the Earth-Moon plane of either 30 or 40 degrees. Note that the trajectories must spend most of the time away from the Earth-Moon plane and near their maximum elongation. Hence, to have the best chances to find Trojan asteroids in the Earth-Moon system one should focus the search around either 30 or 40 degrees over (and under) the Earth-Moon plane. Performing the search on this plane has much less chances of success and, even in this case, it can be difficult to confirm an observation since the asteroid is moving at its highest speed. In fact, there are records of a few observations of small dust clouds near the Earth-Moon Lagrangian points, but none of them was confirmed later [FV80].

## Acknowledgements

This research has been supported by the Spanish CICYT grant BFM2000-0623, the Catalan CIRIT grant 2001SGR-70 and DURSI. The numerical simulations have been done on Hidra, the Beowulf cluster of the UB-UPC Dynamical Systems Group (see <http://www.maia.ub.es/dsg/hidra/>).



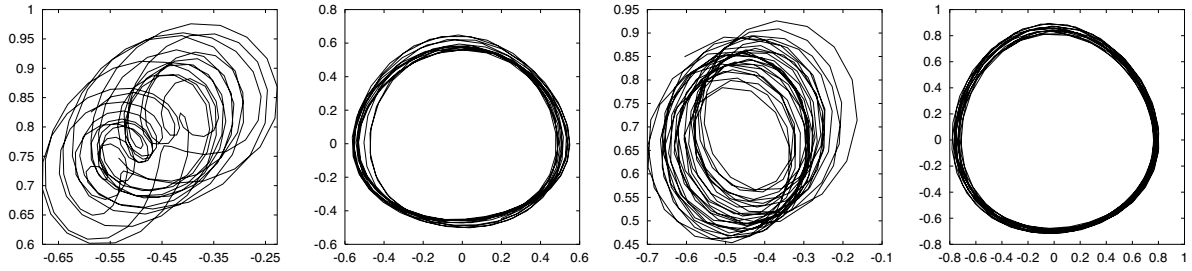


Figure 6: Orbits inside the stable region near  $L_5$ , for the JPL model. First plot:  $(x, y)$  projection of an orbit with  $\dot{z} = 0.58$ . Second plot:  $(z, \dot{z})$  projection of the previous orbit. Third plot:  $(x, y)$  projection of an orbit with  $\dot{z} = 0.83$ . Fourth plot:  $(z, \dot{z})$  projection of the previous orbit. Integration time: 1 year.

## References

- [BFG98] G. Benettin, F. Fassò, and M. Guzzo. Nekhoroshev-stability of  $L_4$  and  $L_5$  in the spatial Restricted Three-Body Problem. *Regul. Chaotic Dyn.*, 3(3):56–72, 1998.
- [CG91] A. Celletti and A. Giorgilli. On the stability of the Lagrangian points in the spatial Restricted Three Body Problem. *Celestial Mech.*, 50(1):31–58, 1991.
- [CJ00] E. Castellà and À. Jorba. On the vertical families of two-dimensional tori near the triangular points of the Bicircular problem. *Celestial Mech.*, 76(1):35–54, 2000.
- [CRR64] J. Cronin, P.B. Richards, and L.H. Russell. Some periodic solutions of a four-body problem. *Icarus*, 3:423–428, 1964.
- [DJS91] C. Díez, À. Jorba, and C. Simó. A dynamical equivalent to the equilateral libration points of the real Earth-Moon system. *Celestial Mech.*, 50(1):13–29, 1991.
- [FV80] R.A. Freitas and F. Valdes. A search for natural or artificial objects located at the Earth-Moon libration points. *Icarus*, 42:442–447, 1980.
- [GDF<sup>+</sup>89] A. Giorgilli, A. Delshams, E. Fontich, L. Galgani, and C. Simó. Effective stability for a Hamiltonian system near an elliptic equilibrium point, with an application to the restricted three body problem. *J. Differential Equations*, 77:167–198, 1989.
- [GJMS93] G. Gómez, À. Jorba, J. Masdemont, and C. Simó. Study of Poincaré maps for orbits near Lagrangian points. ESOC contract 9711/91/D/IM(SC), final report, European Space Agency, 1993.

- [GJMS01] G. Gómez, À. Jorba, J. Masdemont, and C. Simó. *Dynamics and mission design near libration points. Vol. IV, Advanced methods for triangular points*, volume 5 of *World Scientific Monograph Series in Mathematics*. World Scientific Publishing Co. Inc., 2001.
- [Jor00] À. Jorba. A numerical study on the existence of stable motions near the triangular points of the real Earth-Moon system. *Astron. Astrophys.*, 364(1):327–338, 2000.
- [Jor01] À. Jorba. Numerical computation of the normal behaviour of invariant curves of  $n$ -dimensional maps. *Nonlinearity*, 14(5):943–976, 2001.
- [JPL] <http://ssd.jpl.nasa.gov/horizons.html>.
- [JV97a] À. Jorba and J. Villanueva. On the normal behaviour of partially elliptic lower dimensional tori of Hamiltonian systems. *Nonlinearity*, 10:783–822, 1997.
- [JV97b] À. Jorba and J. Villanueva. On the persistence of lower dimensional invariant tori under quasi-periodic perturbations. *J. Nonlinear Sci.*, 7:427–473, 1997.
- [JV01] À. Jorba and J. Villanueva. The fine geometry of the Cantor families of invariant tori in Hamiltonian systems. In *European Congress of Mathematics, Vol. II (Barcelona, 2000)*, volume 202 of *Progr. Math.*, pages 557–564. Birkhäuser, Basel, 2001.
- [SGJM95] C. Simó, G. Gómez, À. Jorba, and J. Masdemont. The Bicircular model near the triangular libration points of the RTBP. In A.E. Roy and B.A. Steves, editors, *From Newton to Chaos*, pages 343–370, New York, 1995. Plenum Press.
- [Sim89] C. Simó. Estabilitat de sistemes Hamiltonians. *Mem. Real Acad. Cienc. Artes Barcelona*, 48(7):303–348, 1989.
- [Sze67] V. Szebehely. *Theory of Orbits*. Academic Press, 1967.